Environmental Earth Sciences (2021) 80:177
https://doi.org/10.1007/s12665-021-09499-5

ORIGINAL ARTICLE

Evaluating the performance of multisource digital elevation models using morphometric parameters and field survey data over the mountainous landscapes of northwest Himalaya, India

Irfan Rashid[1] · **Sadaff Altaf**[1]

Received: 5 November 2020 / Accepted: 10 February 2021 / Published online: 24 February 2021
© The Author(s), under exclusive licence to Springer-Verlag GmbH, DE part of Springer Nature 2021

Abstract
In this study, seven morphometric characteristics were assessed from three freely available multisource DEMs and correlated with extensive field observations to assess the best-fit DEM over the mountainous landscapes of Kashmir Valley, northwest Himalaya, India. The morphometric parameters were assessed using 30 m ASTER GDEM v2 (ASTERDEM), SRTMDEM, and CartoDEM v3 R1 (CARTODEM) in the Ferozpora watershed of the Jhelum Basin, Kashmir Himalaya. Our findings indicated the closeness of mean bifurcation ratio (*Rbm*) values between manual digitization (*Rbm* = 4.12) and CARTODEM (*Rbm* = 4.07). The GPS-based values of drainage basin asymmetry, stream gradient index, basin relief, and longitudinal river profile also indicated a strong resemblance with CARTODEM-derived values. It is hence concluded that CARTODEM is the best-fit DEM representing the topographic and morphometric characteristics over the Kashmir region, however, the results from this analysis need to be tested and validated over larger geographic domains with contrasting lithological and topographic characteristics.

Keywords DEM quality · GPS survey · Basin morphometry · Kashmir himalaya

Introduction

The evolution of a landscape by the formation, modification, or destruction of the landforms is often associated with the structures and processes related to the deformation of the Earth's crust (i.e. tectonics) controlled by endogenic processes (Bull and McFadden 1977). Often referred to as tectonic geomorphology or morphotectonics, describing the relationship between landforms and tectonic activities such as faulting, folding, tilting, upliftment or subsidence and erosion processes (Burbank and Anderson 2001), it is immensely important for identifying and understanding the seismic hazards and for quantifying active and geologically recent tectonic deformations (Ramírez-Herrera 1998; Bahrami 2013). Various studies suggest that morphometric indices can help in ascertaining the geological and geomorphological characterization of an area (Bull and McFadden 1977; Rockwell et al. 1985; Wells et al. 1988; Keller and Pinter 1996; Azor et al. 2002; El Hamdouni et al. 2008; Dehbozorgi et al. 2010).

Quantification of morphometric indices has proven to be useful in the tectonically active regions like the Himalaya by succoring in understanding of the basin characteristics related to the shape, slope, rock hardness, diastrophism and other factors (Strahler 1964; Jackson et al. 1998; Sung and Chen 2004; Ramsey et al. 2008). These indices have been extensively used by gathering the necessary information from the topographic maps, and aerial photographs and continue to be in vogue due to the advancements in the use of satellite remote sensing for topographic mapping (Horton 1945; Keller and Pinter 1996; Wells et al. 1988). Accordingly, seven morphometric indices that include drainage pattern/stream order (U), the bifurcation ratio (*Rb*), drainage basin asymmetry (*AF*), stream length-gradient index (SI), valley floor width to valley height ratio (*Vf*), Basin relief (*H*) and, longitudinal river profiles (LRP) (Bull and McFadden 1977; Pandey and Dubey 2003; Ahmed et al. 2010; Thomas et al. 2010), were assessed using multisource DEMs. Studying these indices for inferring the tectonic activity has enhanced the scientific understanding of various seismically

✉ Irfan Rashid
irfangis@kashmiruniversity.ac.in; irfangis@gmail.com

[1] Department of Geoinformatics, University of Kashmir, Hazratbal Srinagar, Jammu and Kashmir 190006, India

active areas around the world (Rockwell et al. 1985; Wells et al. 1988; Cox 1994; El Hamdouni et al. 2008) incldluing Kashmir Valley (Ahmad and Bhat 2012; 2013; Ahmad et al. 2014, 2018; Dar et al. 2014a). These indices are calculated from the topographic information or can be generated by several techniques like extensive ground surveys, Digital Elevation Models (DEMs) produced from topographic maps, aerial photographs, laser scanning, and Interferometric Synthetic Aperture Radar (InSAR) (Seferciket al. 2007; Sharma et al. 2010).

The morphometric characterization of tectonically active areas has become easier with the emergence of freely available DEMs, advancements in GIS platforms, and the development of advanced GIS algorithms (Verrioset al. 2004; Hayakawa and Oguchi 2006; Font et al. 2010; Ahmad et al. 2018). Moreover, it has been studied that the resolution of DEMs and the technique for acquiring the topographic data significantly affect the accuracy of the processes being simulated (Jenson 1991; Wolock and McCabe 2000; De Vente et al. 2009). Many researchers have identified that the elevational differences in the DEMs are more pronounced in high-relief areas as compared to lower elevations which may lead to misinterpretation of the analysis (Toutin 2002; Hirano et al. 2003; Orvis 2003). Many researchers have also ascribed false heights to landscape elements owing to the lack of knowledge about the datum and/ or ellipsoid/ geoid on which the geographic data is projected (Perez et al. 2006; Apollo et al. 2020). Therefore, it is imperative to have DEMs with similar projection characteristics before going for any comparative quality assessment.

This study evaluates the robustness of three similar-resolution DEMs using seven morphometric characteristics and field-based measurements for the first time over tectonically active Kashmir Himalaya. Although there is a plethora of literature related to the morphotectonics of the region, the suitability of DEMs for tectonic characterization has never been attempted. In this paper, ASTERGDEM, CARTODEM, and SRTMDEM, all with a spatial resolution of 30 m, were used over Kashmir Himalaya, India to ascertain their robustness for tectonic characterization of the region.

Study site description

Jhelum, an asymmetric basin, draining through Kashmir Valley is an oval-shaped basin that lies in the North-West Himalaya between the Pir Panjal Range in the SW and the Greater Himalayan Range in the NE (Romshoo et al. 2017) in the Indian state of Jammu and Kashmir. The Pir Panjal Range comprises a complex faulting pattern including several thrusts (Thakur et al. 2010). The valley comprises of Archean to Recent stratigraphic record of rocks of all ages and is filled with up to 1300 m thick 'Karewa Group' formations which are Plio-Pleistocene fluvio-glaciolacustrine sediments (Bhatt 1975; Kotlia 1985; Dar et al. 2014a). The valley is characterized by numerous springs and 24 main tributaries that drain into the Jhelum River forming the Jhelum basin. The present analysis has been carried out in one of the watersheds of Jhelum, the Ferozpora watershed (Fig. 1). The watershed drains an area of ~ 450 km^2 lying between 33° 54′ 26″–34° 18′ 23″ N lat and 74° 18′ 40″–74° 42′ 25″ E lon with the altitude extremes of 1455 m and 4538 m asl (Rashid et al. 2016). Ferozpora *Nallah*, a tributary of Jhelum drains the upper snow-clad slopes of the Pir Panjal (Dar et al. 2014b) between the Jamianwali Gali and the Apharwat ranges (Rashid et al. 2016). On entering the relatively plain area, Ferozpora *Nallah* gets divided into two branches emptying into the Wular, Asia's largest freshwater lake (Meraj et al. 2018). The Ferozpora *Nallah* has several streams forming a well-developed dendritic drainage pattern in the upper portion of the catchment and more or less parallel drainage pattern in the lower portion (Lawrence 1895; Wadia 1975). Geologically, the area is dominated by the basic volcanic rocks of Panjal traps, Triassic Limestone, Quaternary sediments of Karewa deposits, and alluvium (Middlemiss 1910; Bhatt 1989).

Materials and methods

Datasets and data quality

The datasets used in this research could be broadly classified into four categories that include multisource DEMs, high-resolution basemap imagery of ArcMap 10.1, Google Earth images, and ground data collected from Global Positioning System (GPS). CartoDEM v3 R1 (Cartosat-1 DEM Waterbody Flattened) is an openly accessible National DEM provided by the Indian Space Research Organization (ISRO) with a spatial resolution of 30 m (Baral et al. 2016). Shuttle Radar Topography Mission DEM (SRTMDEM) is a product of a collaborative effort by the National Aeronautics and Space Administration (NASA), the National Imagery and Mapping Agency (NIMA), the German Aerospace Centre (DLR) and Italian Space Agency (ASI). The data has been collected using the InSAR technique at 1 arcsecond (~ 30 m) and 3 arcseconds (~ 90 m) (Rabus et al. 2003; Sharma et al. 2010). Another DEM, ASTER GDEM v2 (Advanced Spaceborne Thermal Emission and Reflection Radiometer) synthesized from the ASTER stereopairs from NASA's Terra spacecraft is available at 30 m (Abrams 2000). Further, drainage was manually delineated from high-resolution basemap imagery of Arc Map 10.1. Handheld Trimble Juno T41/5 with a positional accuracy of ± 8 m was used for in-situ data collection. The logging interval for coordinate data collection was set to 10 s for at least 5 min at a single

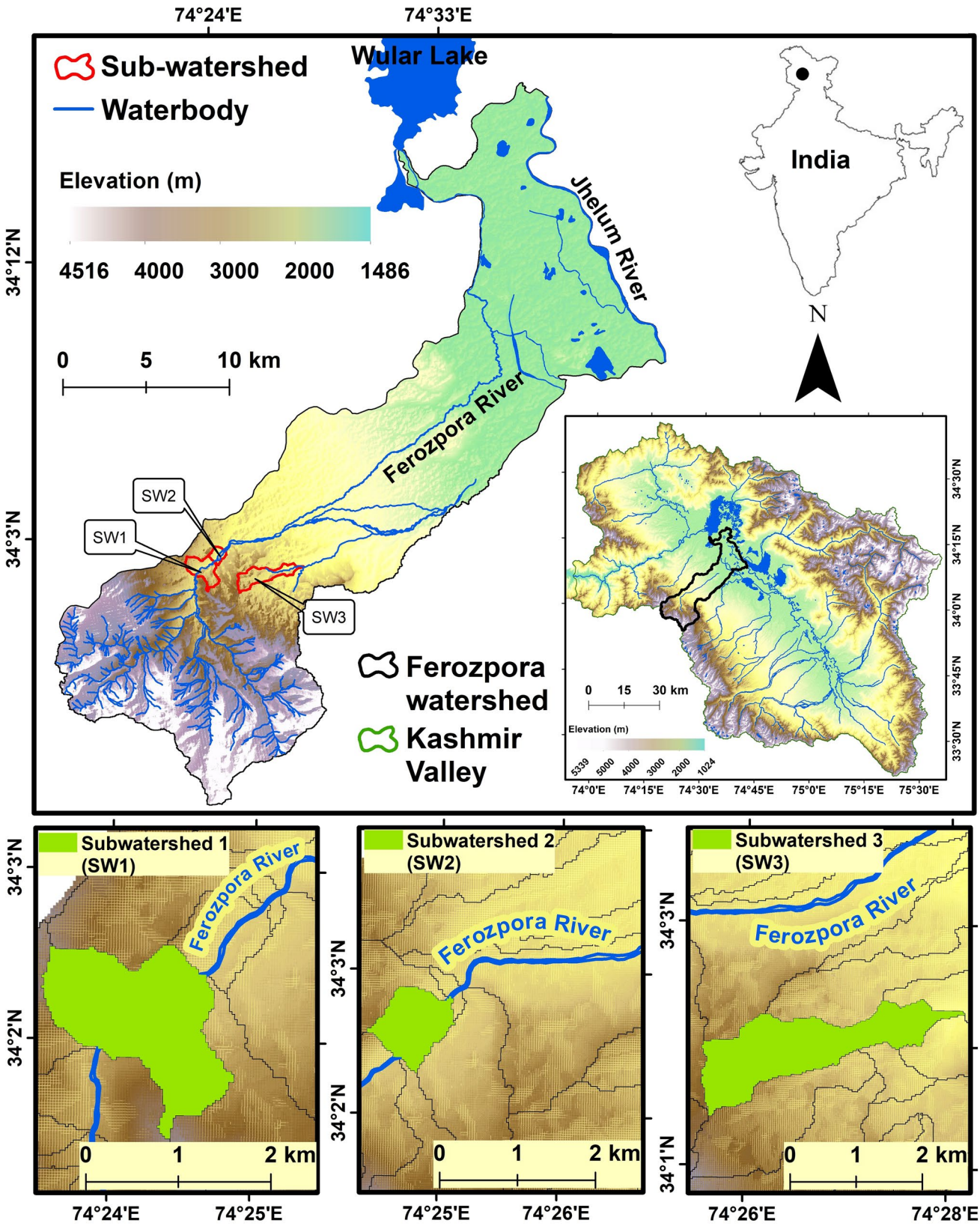

Fig. 1 Location of the study area. Top panel: topographic variability of Ferozpora watershed using CARTODEM along with sub-watersheds, Bottom right: Ferozpora watershed in Kashmir valley. Top right: location of study area with respect to Indian mainland. Bottom panel: zoomed-in view of sub-watersheds

location. Table 1 provides details of the datasets used in this study.

Methods

In the present study, morphometric analysis of seven parameters (U, *Rb*, *AF*, SI, *Vf*, *H* and LRP) has been carried out. The results from morphometric analysis were then compared with the field-based measurements to study the morphotectonics of this region and to check the efficacy of the DEMs for tectonic studies. The automatically derived drainage patterns from coarser-resolution DEMs were validated with the manually delineated drainage patterns from high-resolution satellite data (1:5000 scale). The manual delineation with the cognitive inputs from the analyst was employed given its potential in mapping the geomorphic features in a topographically rugged terrain (Rashid et al., 2016, 2020a, b; Majeed et al. 2021). The DEMs (ASTERDEM, CARTODEM, and SRTMDEM) were used in the GIS environment to generate the boundaries of the sub-watersheds and the drainage pattern by defining a pour point at the outlet of the Ferozpora watershed (Garbrecht and Martz 1997; Tarboton and Shankar 1998; Altaf et al. 2013). The pour point is a location where water drained from the whole of the watershed flows into the main river (Antonić et al. 2001). After that, the drainage network of the Ferozpora watershed was manually digitized using the high-resolution basemap imagery of ArcMap 10.1.

Stream order (U)

For stream ordering, Strahler's Law (Strahler 1952; Schumm 1956; Singh 1980; Romshoo et al. 2012) was followed by designating an unbranched stream as the first-order stream which after joining another first-order stream forms a second-order stream just below the junction. Two second-order streams join together to form third order and so on. The number of streams of each order were counted and recorded. The calculations were carried out for both the automated and manually delineated drainage networks. Therefore, the drainage pattern generated from DEMs was validated with that from the manual digitization to check the closeness of patterns between the two in the Ferozpora watershed.

Bifurcation ratio (*Rb*)

It is defined as the ratio between the total number of stream segments of one order (*Nu*) to that of the next higher (*Nu* + 1) order (Strahler 1957). It is a dimensionless property and was calculated as per the Eq. (1) as:

$$Rb = \frac{Nu}{Nu + 1} \quad (1)$$

The mean bifurcation ratio (*Rbm*), which is the mean of the *Rb* of all the orders, is an indicator of structural complexity and permeability of the terrain and is thus negatively correlated with the permeability of a watershed (Horton 1945). High *Rbm* indicates high structural complexity and an early hydrograph peak with a potential for flash flooding during the storm events which results in the degradation of topsoil (Howard 1990; Rakesh et al. 2000). This *Rbm* was calculated from all the sources and was later on compared with the calculations from manual digitization to check the accuracy of the DEMs.

Drainage basin asymmetry (*AF*)

AF allows determination of the general tilt of the basin landscape, irrespective of whether the tilt is due to local or regional tectonic deformation (Hare and Gardner 1985) and is expressed as per the Eq. (2) as:

Table 1 Details of the datasets used in the study

S. no	Datasets	Spatial resolution	Origin	Weblink for data download/model	Purpose
1	Digital Elevation Models (DEM)				Topographic evaluation
	ASTER GDEM v2	30 m	Optical Stereopairs	https://earthexplorer.usgs.gov/	
	SRTM DEM	30 m	C band SAR	https://earthexplorer.usgs.gov/	
	CARTO DEM v3 R1	30 m	Optical	https://bhuvan.nrsc.gov.in/	
2	High resolution satellite images				Manual delineation of drainage network
	Basemap of ArcMap and Google Earth	~5 m	NA	NA	
3	GPS data				Elevation data for comparison with DEMs
	Field survey points	Point data	Collected in-situ	Trimble Juno T41/5 with an accuracy of ± 8 m	

$$AF = \left(\frac{Ar}{At}\right) \times 100 \quad (2)$$

where AF is the drainage basin asymmetry, At is the total area of the drainage basin, and Ar is the area of the drainage basin to the right side of the trunk channel when facing downstream.

AF was developed for detecting tectonic tilting as the active tectonic deformations form drainage with distinct patterns and geometry. For a stable stream network, AF should be equal to 50. AF greater than 50 suggests that the channel has shifted towards the left side of the channel while the vice versa is true for the values lesser than 50 (Hare and Gardner 1985; Gardner et al. 1987; Ahmad et al. 2014). AF was calculated from the three DEMs for the Ferozpora watershed which was then compared with the AF results from a digitized stream network.

Stream length-gradient index (SI)

This parameter is calculated for a particular stream of interest and correlates to the stream power or differential rock erodibility (Hack 1973). Hydrologically, total stream power available at a particular reach of the channel is important because it is related to the ability of a stream to erode its bed and transport sediment (Azor et al. 2002). The SI is very sensitive to changes in the channel slope and this sensitivity allows the evaluation of relationships among possible tectonic activity, rock resistance, and topography (Keller and Pinter 1996). The stream gradient index (SI) calculated for a particular reach of interest (stream segment) can be computed as per the Eq. (3) as:

$$SL = \frac{\Delta H}{\Delta L} \times L \quad (3)$$

where $\Delta H/\Delta L$ is the channel slope or gradient of the reach, and L is the total channel length from the point of interest where the index is being calculated upstream to the highest point on the channel. For the ΔH, the maximum and minimum elevations were calculated from the highest point of the stream and the center of the ΔL respectively. ΔL is the length of the reach of interest where the index is being calculated. The calculations were carried out for all the DEMs and digitized stream network to check the accuracy of the DEMs.

Valley floor width to valley height ratio (*Vf*)

This index differentiates between broad-floored canyons associated with relatively high values of Vf, and V-shaped valleys associated with relatively lower values (Bull and McFadden 1977; Keller and Pinter 2002). High values of Vf are associated with low uplift rates so that streams cut broad valley floors. Low values of Vf reflect deep valleys with streams that are actively incising, commonly associated with uplift (Keller and Pinter 1996). This index is based on the observation that areas undergoing rapid upliftment are marked by incised streams with narrow valley floors and V-shaped valley profiles. Vf is expressed as per the Eq. (4) as:

$$Vf = \frac{2Vw}{[(Eld - Esc) + (Erd - Esc)]} \quad (4)$$

where Vw is the width of the valley for given profile at fixed length, Erd and Eld are the elevation of right and left divides for a given section line respectively facing downstream and Esc is the elevation of the valley floor. The Vf calculations were carried on a sub-watershed SW3 of the Ferozpora watershed to validate the results from DEMs with the field-based measurements. For the field measurements, 30 elevation values (GCPs) were gathered using the GPS across a transect from one to another ridge of SW3.

Basin relief (*H*)

The elevation difference between the highest and the lowest points on the valley floor of a watershed is referred to as total relief (Schumm 1956). There is a strong correlation between hydrological characteristics and the H of a drainage basin (Dodov and Foufoula-Georgiou 2005). It is an index of overall steepness of a drainage basin as well as of the intensity of erosion processes operating on the slopes of a basin (Dodov and Foufoula-Georgiou 2005) and is expressed as per the Eq. (5) as:

$$H = H_{\max} - H_{\min} \quad (5)$$

where $H_{\max}$ is maximum elevation and $H_{\min}$ is the maximum elevation of the basin. The calculations were carried out on SW2 sub-watershed of the Ferozpora watershed using the three DEMs, and the field measurements. A continuous stream of points was acquired along the main stream of SW2 using the GPS for the field-based measurements. Then the basin relief was calculated using the maximum and minimum elevation values from all the sources to check the efficacy of DEMs in representing the H.

Longitudinal river profile (LRP)

Rivers that are not tectonically perturbed typically develop a smoothly changing, concave longitudinal profile (Zuchiewicz 1980). Departures of the river gradient from this ideal smooth shape may reflect variations in the lithology of the river bed, or tectonic activity (Mackin 1948; Turowskiet al. 2009). Rivers that are tectonically disturbed are predicted to approach a gradient profile rapidly (Snow and Slingerland 1987) once such disturbance ceases. Thus,

perturbations in river profiles may be interpreted as a response to ongoing tectonism. The plotting of longitudinal profiles shows altitude against distance downstream. It represents the channel gradient of the river from its source to the mouth. LRP was generated by plotting a histogram between the river length and the elevation of the Ferozpora watershed to study the tectonic signatures in the area. The results were validated with the field-based measurements wherein the LRPs of the two sub-watersheds SW1 and SW2 of the Ferozpora watershed were generated using the GPS surveys. A continuous stream of 180 GCPs for the elevation measurements were taken along the main streams draining the SW1 and SW2 which were then plotted against the length of these rivers. The GPS-based LRP was then compared with the LRPs of SW1 and SW2 generated from the DEMs for the same river segment.

Results

This study involved use of seven morphometric parameters and field-based GPS observations to evaluate the quality of 3 multisource DEMs.

The stream order (U) of the Ferozpora watershed was delineated from the three DEMs and a high-resolution image as shown in Fig. 2. The drainage network showed that the stream order going to 5th order streams. The highest synonymity in the pattern was observed in the streams generated from the CARTODEM when compared to the manually digitized streams especially the 5th order. The streams showed a somewhat similar pattern up to the 4th order in all the DEMs and deviation in the 5th order. The 5th order stream in all the DEMs and high-resolution imagery were observed in the lower plains of the watershed. It is hence obvious that the rivers are best represented by the CARTODEM.

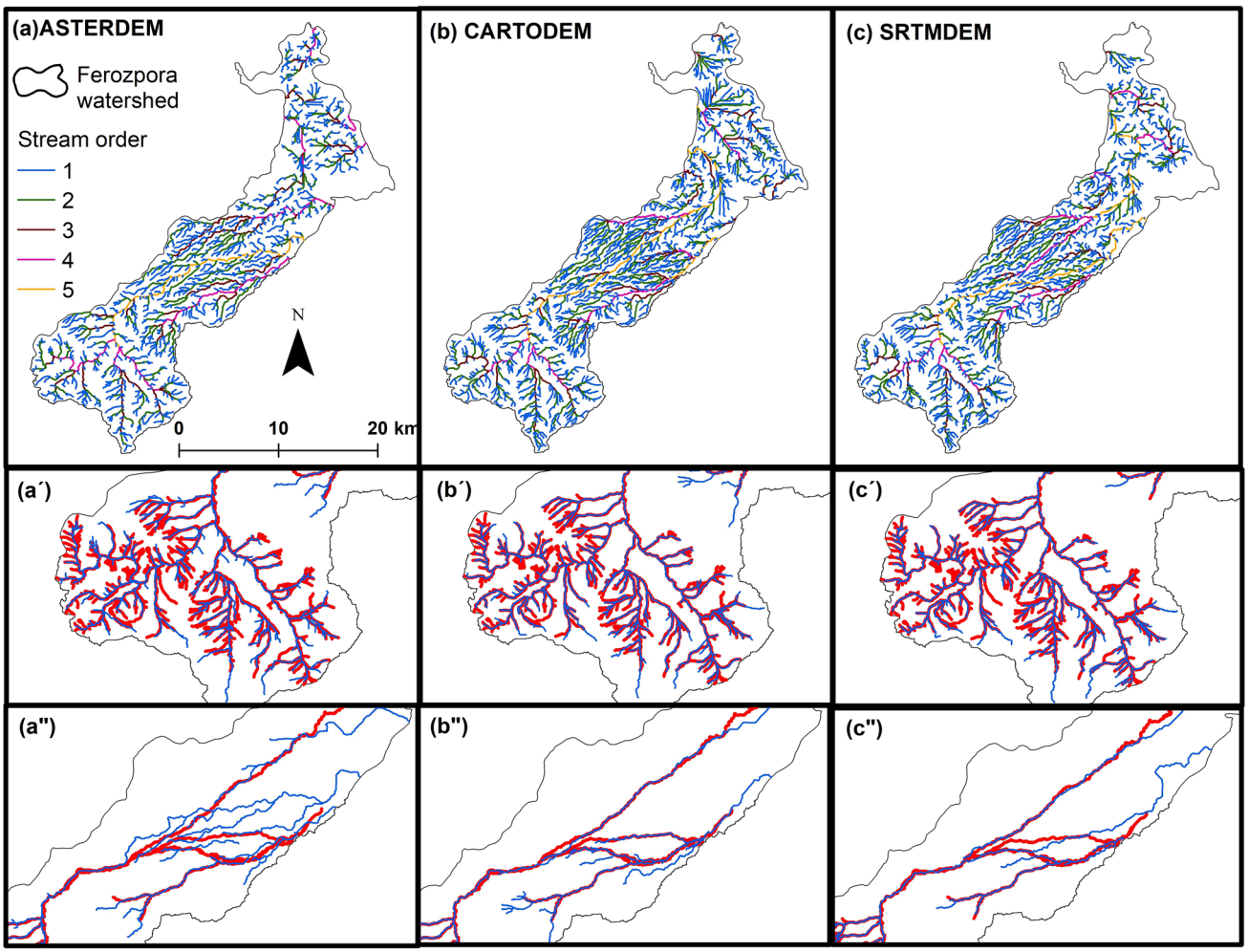

Fig. 2 Stream order of Ferozpora watershed as delineated from (**a**) ASTERDEM; **b** CARTODEM; **c** SRTMDEM; **a′**–**c′** Comparison of manually digitized drainage (in Red) with the DEM derived drainage patterns at higher region; **a″**–**c″** Comparison of manually digitized drainage (in Red) with the DEM derived drainage patterns at planar region

The bifurcation ratio (*Rb*) generated from the streams of high-resolution imagery and DEMs showed close resemblance in all the stream orders. The mean bifurcation ratio (*Rbm*) showed the closest resemblance in streams generated from CARTODEM compared to manually digitized streams followed by SRTMDEM. Rbm in the Ferozpora watershed is 4.12, 5.44, 4.07, and 4.39 for the digitized streams and streams derived from ASTERDEM, CARTODEM, and SRTMDEM respectively (Table 2).

The parameters used for the calculation of *AF* for the Ferozpora watershed are shown in Fig. 3. The analysis of drainage basin asymmetry (*AF*) for the Ferozpora watershed indicated ASTERDEM and SRTMDEM show values less than 50 i.e. 31 and 27 respectively, indicating that the channel downstream has shifted towards the right side of the basin. On the contrary, calculations from the CARTODEM ($AF = 63$) reveal that the channel has shifted towards the left side. The calculations cohere with the outputs from the digitized stream network generated from high-resolution imagery. Thus, indicating that the results from CARTODEM are closer to reality than the other two DEMs (Table 3).

The higher values of SI from the SRTMDEM (863.4), CARTODEM (632.2), and ASTERDEM (423.9) indicate higher tectonic activity in the Ferozpora watershed (Table 4). Our calculations from the GPS data also revealed high tectonic activity (SI = 742.9) which demonstrated the closest resemblance to the values from CARTODEM followed by SRTMDEM indicating that the CARTODEM shows better results than the other two DEMs (Fig. 4).

The *Vf* calculations carried out for sub-watershed SW3 using the valley cross-section are shown in Fig. 5a, b. The results revealed that all the DEMs indicate SW3 is a U-shaped with lesser tectonic activity. On contrary, field-based GPS measurements showed that SW3 is V-shaped with higher tectonic activity (Table 5).

H was specifically used to check the robustness of DEMs in capturing the highest and lowest elevation of a mountainous watershed. For this parameter, the analysis was carried out on SW2 sub-watershed over a continuous stream of 65 points using a GPS. These points were further compared with the elevation values of DEMs at the respective locations. The results showed that CARTODEM ($H = 39$) showed the closest resemblance to the GPS-acquired relief ($H = 35$) values (Table 6).

As shown in Fig. 6, the LRP of Ferozpora showed a steep slope at the source followed by the decreasing gradient in all the DEMs which converges to a convex depression particularly within the resistant lithology of the Panjal trap from 1–3 km. The river has a steep slope up to 10 km which becomes gentle from 10–30 km and planar beyond 30 km in all DEMs. To check the accuracy of the DEMs, 2 sub-watersheds of the Ferozpora watershed, SW1 and SW2 shown in Fig. 7a, b respectively, were taken into account. It was observed that the elevation values collected using GPS showed the closest resemblance to the elevation values of the CARTODEM in both the sub-watersheds.

Table 2 Bifurcation ratio (Rb) values of the Ferozpora watershed

Data Source	Stream order	Number of streams	Bifurcation ratio (*Rb*)	*Rbm*
Digitized	1	269	–	
	2	63	4.27	
	3	15	4.20	4.12
	4	3	5.00	
	5	1	3.00	
ASTERDEM	1	696	–	5.44
	2	164	4.24	
	3	36	4.55	
	4	9	4.00	
	5	1	9.00	
CARTODEM	1	797	–	4.07
	2	179	4.45	
	3	48	3.72	
	4	10	4.80	
	5	3	3.34	
SRTMDEM	1	743	–	4.39
	2	166	4.47	
	3	37	4.48	
	4	9	4.11	
	5	2	4.50	

Discussion

The DEM quality in the tectonically active Kashmir Himalaya (Bhat 1982; Schiffman et al. 2013; Mir et al. 2017) was assessed using morphometric parameters and field data. While all the 7 morphometric parameters, were specifically analyzed to identify the best-fit DEM, the 5 parameters that include *Rb*/*Rbm*, *AF*, SI, *Vf*, and LRP provided some insights into the tectonic behavior of the Ferozpora watershed. The analysis shows that streams up to 5th order could be delineated from both the DEMs as well as manual digitization from the high-resolution satellite data. It is pertinent to mention that the properties of the stream networks are very important to study basin characteristics (Strahler 2002). It has been demonstrated that higher the number of stream segments in a particular basin higher will be the order of streams (Shreve 1966; Saran et al. 2010). The higher order of the streams infers high drainage density (Godsey and Kirchner 2014) controlled by the rock types (Tucker et al. 2001; Sangireddy et al. 2016), vegetation cover (Istanbulluoglu and Bras 2005; Hooshyar et al. 2019), and slope (Tucker and Bras 1998; Schneider et al. 2017). It was observed that the

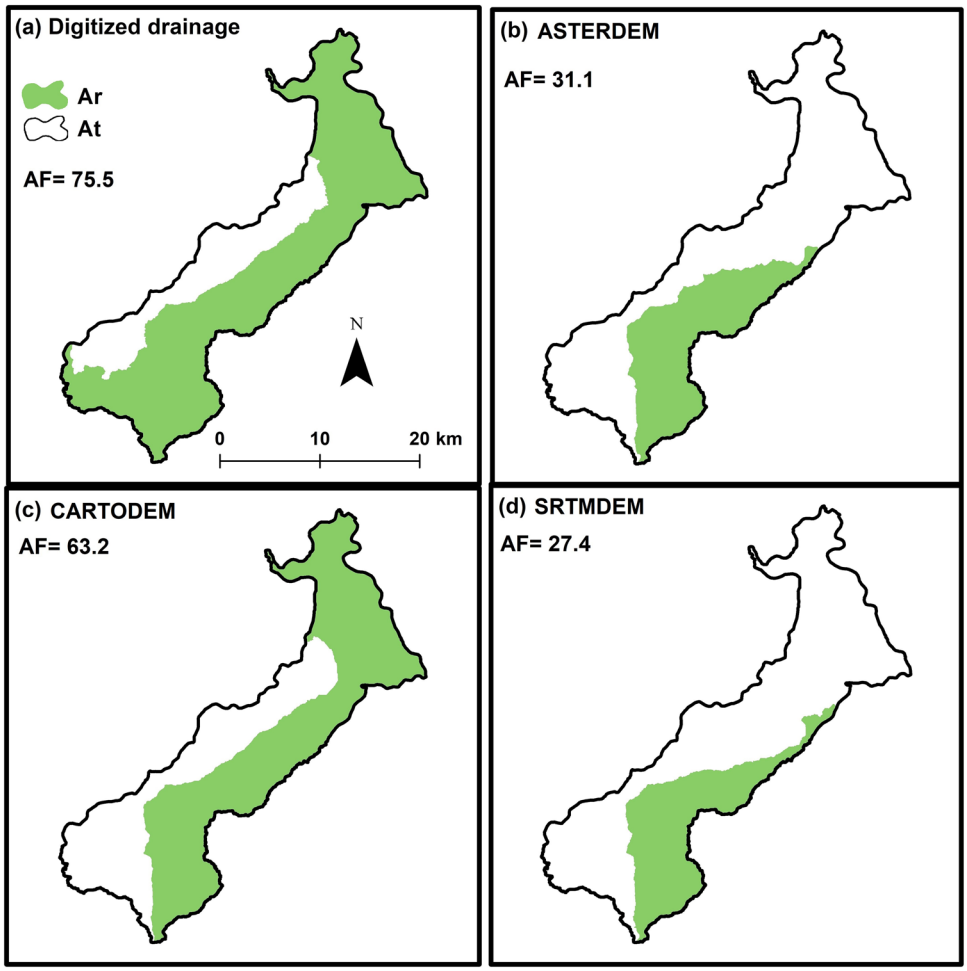

Fig. 3 Parameters used for calculation of *AF* of the Ferozpora watershed. *At*—Total basin area and *Ar*—Area of drainage basin to the right side of trunk channel when facing downstream

Table 3 Drainage basin asymmetry (*AF*) of the Ferozpora watershed

Source	*Ar* (km^2)	*At* (km^2)	*AF*
GPS	336.6	445.8	75.5
ASTERDEM	138.4	445.8	31.1
CARTODEM	281.8	445.8	63.2
SRTMDEM	122.0	445.8	27.4

stream pattern is best represented by CARTODEM, however, none of the DEMs highlighted the bifurcation of the streams in the 5th order. Similarly, the parameter H confirms that the elevation values of CARTODEM showed the closest resemblance to the GPS-acquired values also observed by Rawat et al. (2019).

The *Rbm* from the manually digitized streams, CARTODEM and SRTMDEM indicated values between 4 and 5 indicating tectonic stability compared to that of ASTERDEM (*Rbm* = 5.44) indicating some tectonic activity. The Rbm values for tectonically stable watershed ranges from 3–5 indicating that the geologic structures do not distort the drainage pattern (Bali et al. 2012; Dar et al. 2014a). The Rbm as calculated from all the four sources (viz., three DEMs, and manual delineation) is less than 5 in all the stream orders except for the 4th and 5th order stream generated from the ASTERDEM. The Rbm in the 5th order

Table 4 Stream gradient index (SI) of the Ferozpora watershed. $\Delta L = 2009$ m

Data Source	Elevation (m)		ΔH (m)	$\Delta H/\Delta L$	L (m)	SI (m)
	Maximum	Minimum				
GPS	2202	2127	75	0.04	19,776.9	742.9
SRTMDEM	2253	2158	95	0.05	18,258.33	863.4
CARTODEM	2202	2126	76	0.04	16,711.2	632.2
ASTERDEM	2234	2186	48	0.02	17,743.65	423.9

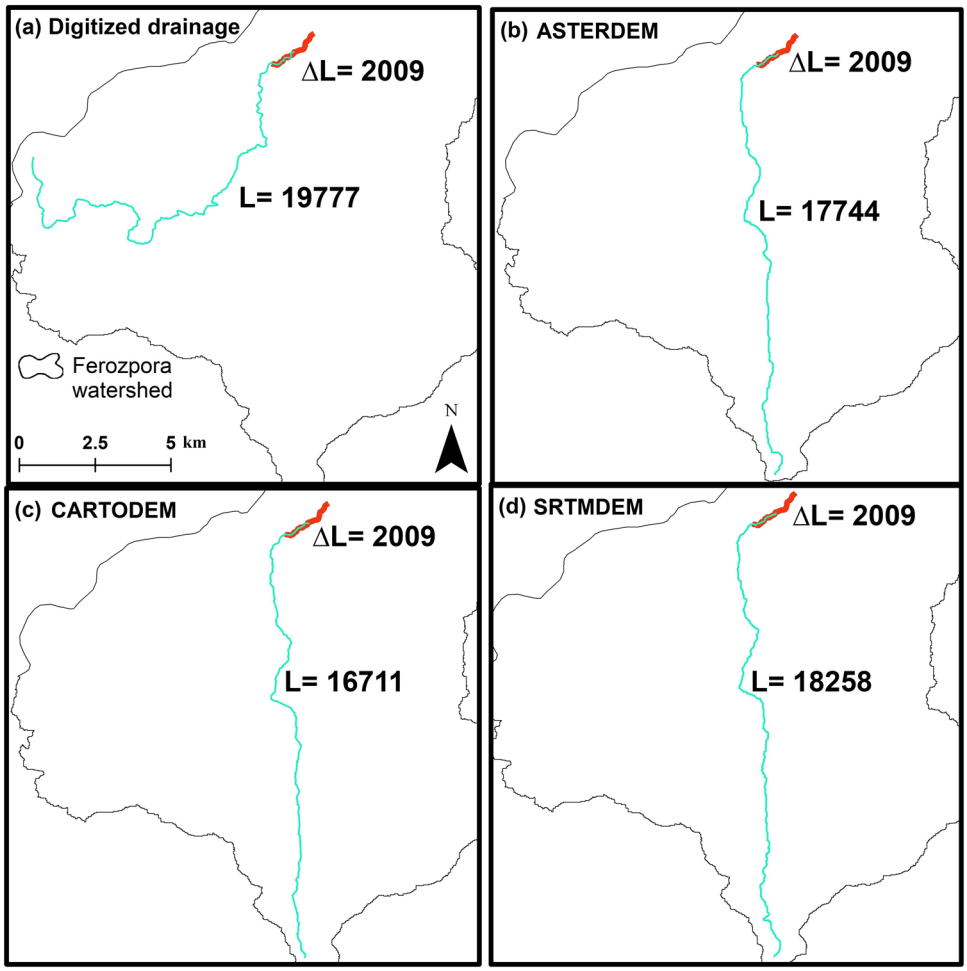

Fig. 4 Parameters used for calculation of SI of the Ferozpora watershed. ΔL—portion of the channel where the index is being calculated and L—total channel length from the point of interest where the index is being calculated upstream to the highest point on the channel

of streams from ASTERDEM is 9 because the DEM has delineated nine 4th-order streams which converge into one 5th order thus reflecting the structural disturbance in the area which is contrary to results from manual delineation and the other two DEMs indicating the possible source of error in ASTERDEM (Gesch et al. 2012). Moreover, the parameter *AF* has been developed for detecting tectonic tilting as the active tectonic deformations form drainage with distinct patterns and geometry. While the results from ASTERDEM and SRTMDEM show that the Ferozpora watershed has shifted towards the right side of the basin, the CARTODEM and digitized stream networks on contrary revealed that the channel has shifted towards the left side. It indicates that the results from CARTODEM are closer to reality than the other two DEMs. Irrespective of the direction of tilting, an *AF* factor deviating from value 50 suggests the active tectonics or structural control (El Hamdouni et al. 2008) in the Ferozpora watershed.

The higher values of the SI from the GPS-based observations, SRTMDEM, CARTODEM, and ASTERDEM indicated that the streams of the watershed cross hard rock terrain associated with high tectonic activity (Hack 1973; Keller and Pinter 2002). The field-based measurements showed the closest resemblance to CARTODEM and the highest deviation from the ASTERDEM (Table 4). For assessing the shape of the SW3, the *Vf* results from all the DEMs indicated a U-shaped valley with lesser tectonic activity in the area. The field-based GPS measurements showed SW3 is a V-shaped valley. This could be an artifact of DEM resolution over the mountainous SW3 subwatershed (Kervyn et al. 2008). The LRP of the Ferozpora watershed shows the convergence of steep slope to a convex depression within the resistant lithology of the Panjal trap at the source indicating signatures of tectonic activity in the region (Ahmad et al. 2014). For the DEM accuracy, elevation values from the GPS showed the closest resemblance to the values of CARTODEM (Fig. 7).

Our analysis suggested that the values of *AF*, SI, and LRP infer tectonic control prevailing over the study area. It is pertinent to mention that the Pir Panjal range has a complex pattern of faulting with the superposition of several thrusts, one of which crosses through the Ferozpora watershed as shown by Shah (2015). This research suggests that CARTODEM is the best DEM representing the morphometric parameters

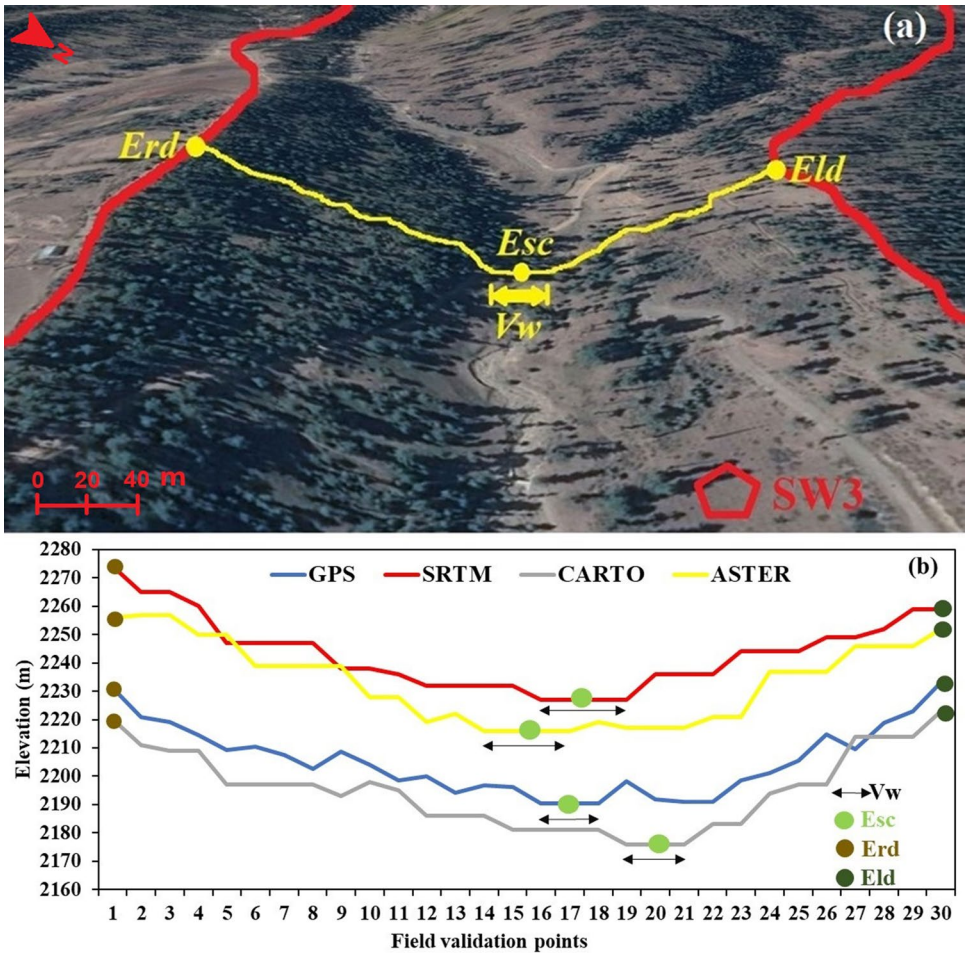

Fig. 5 **a** Transect used for calculation of *Vf*; **b** *Vf* calculations for the transect (where *Vw* width of the valley for given profile at fixed length; *Erd* and *Eld* the elevation of right and left divide; *Esc* elevation of the valley floor)

Table 5 Valley floor width to valley height ratio (*Vf*) of SW3

Data source	*Erd* (m)	*Esc* (m)	*Eld* (m)	*Vw* (m)	*VF*
GPS	2231	2177	2233	20.1	0.37
ASTERDEM	2256	2216	2252	33.5	0.88
CARTODEM	2220	2181	2223	35.4	0.87
SRTMDEM	2274	2227	2259	35.8	0.91

Table 6 Basin relief of SW2

Data source	Elevation (m)		Basin relief (m)
	Maximum	Minimum	
GPS	2158	2123	35
ASTERDEM	2202	2180	22
CARTODEM	2159	2120	39
SRTMDEM	2200	2155	45

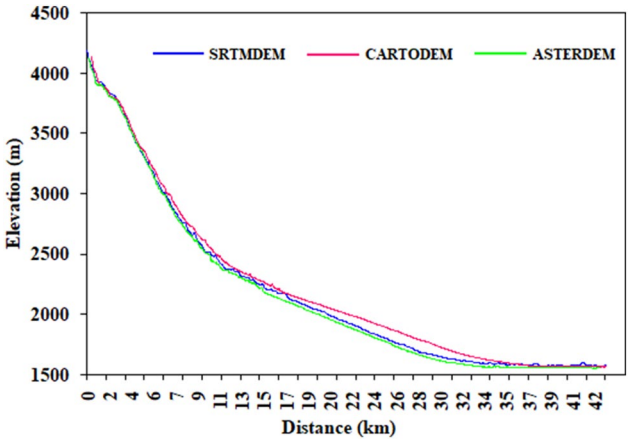

Fig. 6 LRP of Ferozpora watershed based on different DEMs: **a** ASTER; **b** CARTO; **c** SRTM

almost coinciding with the values of field-based GPS measurements. Similar assumptions have been made by various researchers like Evans et al. (2008) for Utah, USA, Mukhejee et al. (2013), and Das and Pardeshi (2018) for various

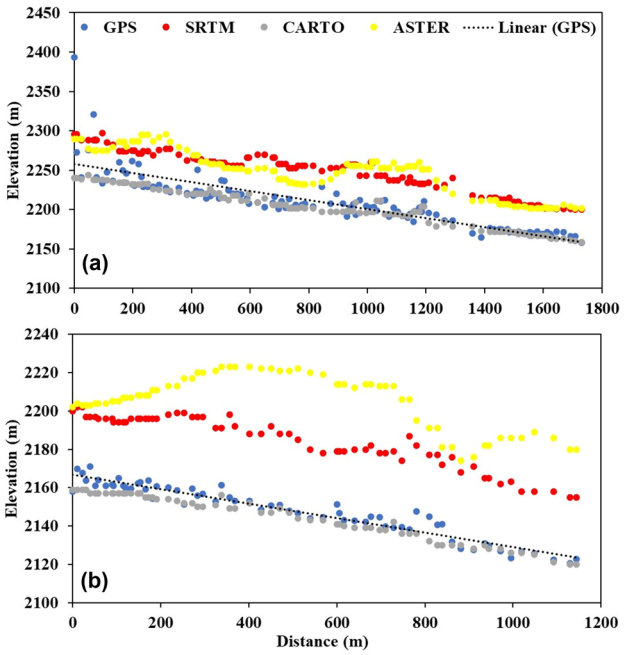

Fig. 7 **a** LRP for SW1; **b** LRP for SW2

parts of India. However, other research findings suggest that CARTODEM has lesser accuracy than ASTERDEM and SRTMDEM (Krishnan et al. 2016; Singh et al. 2016). The findings of this study need to be upscaled to different geological and topographic regimes of the Himalaya to ascertain the best-fit DEM utilizing robust ground-based GPS surveys.

Conclusion

This study offers one of the unique approaches to ascertain the robustness of freely available DEMs using GPS surveys and morphometric indices as proxies over the mountainous Kashmir Himalaya, India. The study assumes importance given that many researchers have widely been using the DEMs for quantifying the tectonic behavior of the Kashmir region without ascertaining the suitability and appropriateness of DEMs for morphotectonic characterization. This study is a first attempt to ascertain DEM quality using morphometric parameters as proxies together with GPS-based field observations in the topographically complex Kashmir Himalayan region. This study is also relevant since vast areas across the Himalayan arc in general and Kashmir region in particular lie in the highest earthquake risk zones (Zone 4 and Zone 5). The analysis using 7 morphometric parameters indicated the robustness of CARTODEM in closely matching the reality (GPS-based measurements and manual digitization from high-resolution imagery). The *Vf* factor however showed a pronounced bias which could be attributed to the spatial resolution of DEMs in comparison to point data as collected using GPS. Further, certain parameters like *AF*, SI, and LRP suggested that the area is tectonically active while Rbm and *Vf* suggested stable behavior of the watershed. Although this research suggested that CARTODEM showed closest match with the field-based GPS observations for the Ferozpora watershed, many other researchers have pointed out caveats related to the accuracy of this DEM. It is, therefore, suggested that the robustness of these DEMs need to be assessed in contrasting lithological and topographic regimes using extensive ground surveys to find the best-fit DEM and its application in ascertaining the tectonic behavior of seismically active regions across mountain regions in general and the Himalaya in particular.

Funding This research did not receive any funding.

Compliance with ethical standards

Conflicts of interest The authors declare that there are no conflicting/competing interests.

References

Abrams M (2000) The advanced spaceborne thermal emission and reflection radiometer (ASTER): data products for the high spatial resolution imager on NASA's Terra platform. Int J Remote Sens 21(5):847–859

Ahmad S, Bhat MI (2012) Tectonic geomorphology of the Rambiara basin, SW Kashmir valley reveals emergent out-of-sequence active fault system. Himalayan Geol 33(2):162–172

Ahmad S, Bhat MI (2013) Investigating drainage response to the Balapur fault interaction on the northeastern PirPanjal flank, Kashmir valley, India. J Himalayan Ecol Sustain Dev 8:121–137

Ahmad S, Bhat MI, Madden C, Bali BS (2014) Geomorphic analysis reveals active tectonic deformation on the eastern flank of the Pir Panjal Range, Kashmir Valley. India Arabian J Geosci 7(6):2225–2235

Ahmad S, Alam A, Ahmad B, Afzal A, Bhat MI, Bhat MS, Ahmad HF (2018) Tectono-geomorphic indices of the Erin basin, NE Kashmir valley, India. J Asian Earth Sci 151:16–30

Ahmed SA, Chandrashekarappa KN, Raj SK, NischithaV KG (2010) Evaluation of morphometric parameters derived from ASTER and SRTM DEM—a study on Bandihole sub-watershed basin in Karnataka. J Indian Soc Remote Sensing 38(2):227–238

Altaf F, Meraj G, Romshoo SA (2013) Morphometric analysis to infer hydrological behaviour of Lidder watershed, Western Himalaya, India. Geogr J. 178021. https://doi.org/10.1155/2013/178021

Antonić O, Hatic D, Pernar R (2001) DEM-based depth in sink as an environmental estimator. Ecol Model 138(1–3):247–254

Apollo M, Mostowska J, Maciuk K, Wengel Y, Jones TE, Cheer JM (2020) Peak-bagging and cartographic misrepresentations: a call to correction. Curr Issues Tourism 1–6. https://doi.org/10.1080/13683500.2020.1812541

Azor A, Keller EA, Yeats RS (2002) Geomorphic indicators of active fold growth: South Mountain-Oak Ridge anticline, Ventura basin, southern California. Geol Soc Am Bull 114(6):745–753

Bahrami S (2013) Tectonic controls on the morphometry of alluvial fans around Danehkhoshk anticline, Zagros. Iran Geomorphology 180:217–230

Bali R, Agarwal KK, Ali SN, Rastogi SK, Krishna K (2012) Drainage morphometry of Himalayan Glacio-fluvial basin, India: hydrologic and neotectonic implications. Environ Earth Sci 66(4):1163–1174

Baral SS, Das J, Saraf AK, Borgohain S, Singh G (2016) Comparison of Cartosat, ASTER and SRTM DEMs of different terrains. Asian J Geoinform 16(1):1–7

Bhat MI (1982) Thermal and tectonic evolution of the Kashmir basin vis-a-vis petroleum prospects. Tectonophysics 88(1–2):117–132

Bhatt DK (1975) On the Quaternary geology of Kashmir Valley with special reference to stratigraphy and sedimentation. Geol Survey of India Misc Publ 24(1):188–203

Bhatt DK (1989) Lithostratigraphy of Karewa Group, Kashmir Valley, India and a critical review of its fossil record. Geol Survey of India 122:1–85

Bull WB, McFadden LD (1977) Tectonic geomorphology north and south of the Garlock Fault, California, in arid regions. A proceedings volume of the eighth annual geomorphology symposium. State University New York, Binghamton, pp 15–138

Burbank DW, Anderson RS (2001) Tectonic geomorphology. Dep Geosci, The Pennsylvania State Univ 140(2):284–291

Cox RT (1994) Analysis of drainage-basin symmetry as a rapid technique to identify areas of possible Quaternary tilt-block tectonics: an example from the Mississippi Embayment. Geol Soc Am Bull 106(5):571–581

Dar RA, Romshoo SA, Chandra R, Ahmad I (2014a) Tectono-geomorphic study of the Karewa Basin of Kashmir Valley. J Asian Earth Sci 92:143–156

Dar RA, Rashid I, Romshoo SA, Marazi A (2014b) Sustainability of winter tourism in a changing climate over Kashmir Himalaya. Environ Monit Assess 186(4):2549–2562

Das S, Pardeshi SD (2018) Comparative analysis of lineaments extracted from Cartosat, SRTM and ASTER DEM: a study based on four watersheds in Konkan region. India Spatial Inform Res 26(1):47–57

De Vente J, Poesen J, Govers G, Boix-Fayos C (2009) The implications of data selection for regional erosion and sediment yield modelling. Earth Surf Proc Land 34(15):1994–2007

Dehbozorgi M, Pourkermani M, Arian M, Matkan AA, Motamedi H, Hosseiniasl A (2010) Quantitative analysis of relative tectonic activity in the Sarvestan area, central Zagros. Iran Geomorphology 121(3–4):329–341

Dodov B, Foufoula-Georgiou E (2005) Fluvial processes and streamflow variability: interplay in the scale-frequency continuum and implications for scaling. Water Resour Res 41(5):W05005

El Hamdouni R, Irigaray C, Fernández T, Chacón J, Keller EA (2008) Assessment of relative active tectonics, southwest border of the Sierra Nevada (Southern Spain). Geomorphology 96(1–2):150–173

Evans GA, Ramachandran B, Zhang Z, Bailey GB, Cheng P (2008) An accuracy assessment of CartoSat-1 stereo image data-derived digital elevation models: a case study of the Drum Mountains, Utah. The Int Arch Photogrammetry, Remote Sensing and Spatial Inform Sci 37(B1):1161–1164

Font M, Amorese D, Lagarde JL (2010) DEM and GIS analysis of the stream gradient index to evaluate effects of tectonics: the Normandy intraplate area (NW France). Geomorphology 119(3–4):172–180

Garbrecht J, Martz LW (1997) The assignment of drainage direction over flat surfaces in raster digital elevation models. J Hydrol 193(1–4):204–213

Gardner TW, Back W, Bullard TF, Hare PW, Kesel RH, Lowe DR, Menges CM, Mora SC, Pazzaglia FJ, Sasowsky ID, Troester JW (1987) Central America and the Caribbean. Geomorphic systems of North America: Boulder, Colorado, Geol Soc Am, Centennial Spec 2:343–402

Gesch D, Oimoen M, Zhang Z, Meyer D, Danielson J (2012) Validation of the ASTER global digital elevation model version 2 over the conterminous United States. Int Arch Photogramm Remote Sensing Spatial Inform Sci 39:B4

Godsey SE, Kirchner JW (2014) Dynamic, discontinuous stream networks: hydrologically driven variations in active drainage density, flowing channels and stream order. Hydrol Process 28(23):5791–5803

Hack JT (1973) Stream-profile analysis and stream-gradient index. J Res US Geol Survey 1(4):421–429

Hare PW, Gardner TW (1985) Geomorphic indicators of vertical neotectonism along converging plate margins, Nicoya Peninsula, Costa Rica. Tectonic Geomorphology 4:75–104

Hayakawa YS, Oguchi T (2006) DEM-based identification of fluvial knickzones and its application to Japanese mountain rivers. Geomorphology 78(1–2):90–106

Hirano A, Welch R, Lang H (2003) Mapping from ASTER stereo image data: DEM validation and accuracy assessment. ISPRS J Photogrammetry and Remote Sensing 57(5–6):356–370

Hooshyar M, Singh A, Wang D, Foufoula-Georgiou E (2019) Climatic controls on landscape dissection and network structure in the absence of vegetation. Geophys Res Lett 46(6):3216–3224

Horton RE (1945) Erosional development of streams and their drainage basins; hydrophysical approach to quantitative morphology. Geol Soc Am Bull 56(3):275–370

Howard AD (1990) Role of hypsometry and planform in basin hydrologic response. Hydrol Process 4(4):373–385

Istanbulluoglu E, Bras RL (2005) Vegetation-modulated landscape evolution: Effects of vegetation on landscape processes, drainage density, and topography. J Geophys Res: Earth Surf 110(F2). https://doi.org/10.1029/2004JF000249

Jackson J, Dissen R, Berryman K (1998) Tilting of active folds and faults in the Manawatu region, New Zealand: evidence from surface drainage patterns. NZ J Geol Geophys 41(4):377–385

Jenson SK (1991) Applications of hydrologic information automatically extracted from digital elevation models. Hydrol Process 5(1):31–44

Keller EA, Pinter N (1996) Active tectonics, vol 19. Prentice Hall, Upper Saddle River, NJ, p 359

Keller EA, Pinter N (2002) Active tectonics: earthquakes, uplift, and landscape, 2nd edn. Englewood Cliffs Prentice Hall, New Jersey, p 362

Kervyn M, Ernst GGJ, Goossens R, Jacobs P (2008) Mapping volcano topography with remote sensing: ASTER vs. SRTM Int J of Remote Sensing 29(22):6515–6538

Kotlia BS (1985) Vertebrate fossils and palaeoenvironment of the Karewa Intermontane Basin, Kashmir, northwestern India. Curr Sci 54(24):1275–1277

Krishnan S, Sajikumar N, Sumam KS (2016) DEM generation using Cartosat-I stereo data and its comparison with publically available DEM. Procedia Technology 24(7):295–302

Lawrence WR (1895) The valley of Kashmir. Chinar Publishing House, Srinagar

Mackin JH (1948) Concept of the graded river. Geol Soc Am Bull 59(10/0016):7606

Majeed U, Rashid I, Sattar A, Allen S, Stoffel M, Nüsser M, Schmidt S (2021) Recession of Gya Glacier and the 2014 glacial lake outburst flood in the Trans-Himalayan region of Ladakh. India Sci Total Environ 756:144008

Meraj G, Romshoo SA, Ayoub S, Altaf S (2018) Geoinformatics based approach for estimating the sediment yield of the mountainous watersheds in Kashmir Himalaya. India Geocarto Int 33(10):1114–1138

Middlemiss CS (1910) A revision of the Silurian-Trias sequence in Kashmir. Geological Survey of India Records 40:206–260
Mir RR, Parvez IA, Gaur VK, Chandra R, Romshoo SA (2017) Crustal structure beneath the Kashmir Basin adjoining the western Himalayan syntaxis. Bull Seismol Soc Am 107(5):2443–2458
Mukherjee S, Joshi PK, Mukherjee S, Ghosh A, Garg RD, Mukhopadhyay A (2013) Evaluation of vertical accuracy of open source digital elevation model (DEM). Int J Appl Earth Obs Geoinform 21:205–217
Orvis KH (2003) The highest mountain in the Caribbean: controversy and resolution via GPS. Carib J Sci 39(3):378–380
Pandey AC, Dubey CS (2003) Terrain mapping and evaluation in Himalayas using remote sensing And GIS techniques—a case study from Tehri Dam and its environs. Int Arch Photogramm Remote Sensing Spatial Inform Sci 34(7/A):650–653
Perez OJ, Hoyer M, Hernández J, Rodríguez C, Marques V, Sue N, Velandia J, Fernandes J, Deiros D (2006) GPS height measurement of Peak Bolivar. Venezuela Survey Review 38(302):697–702
Rabus B, Eineder M, Roth A, Bamler R (2003) The shuttle radar topography mission-a new class of digital elevation models acquired by spaceborne radar. ISPRS J Photogramm Remote Sensing 57(4):241–262
Rakesh K, Lohani AK, Sanjay K, Chattered C, Nema RK (2000) GIS based morphometric analysis of Ajay river basin upto Srarath gauging site of South Bihar. J Appl Hydrol 14(4):45–54
Ramírez-Herrera TM (1998) Geomorphic assessment of active tectonics in the Acambay Graben, Mexican volcanic belt. Earth Surface Process Landforms: J British Geomorphol Group 23(4):317–332
Ramsey LA, Walker RT, Jackson J (2008) Fold evolution and drainage development in the Zagros mountains of Fars province. SE Iran Basin Research 20(1):23–48
Rashid I, Romshoo SA, Hajam JA, Abdullah T (2016) A semi-automated approach for mapping geomorphology in mountainous terrain, Ferozpora watershed (Kashmir Himalaya). J Geol Soc India 88(2):206–212
Rashid I, Majeed U, Aneaus S, Pelto M (2020a) Linking the recent glacier retreat and depleting streamflow patterns with land system changes in Kashmir Himalaya. India Water 12(4):1168
Rashid I, Majeed U, Aneaus S, Cánovas JAB, Stoffel M, Najar NA, Bhat IA, Lotus S (2020b) Impacts of erratic snowfall on apple orchards in Kashmir Valley. India Sustainability 12(21):9206
Rawat KS, Singh SK, Singh MI, Garg BL (2019) Comparative evaluation of vertical accuracy of elevated points with ground control points from ASTERDEM and SRTMDEM with respect to CARTOSAT-1DEM. Remote Sensing Appl: Soc Environ 13:289–297
Rockwell TK, Keller EA, Johnson DL (1985) Tectonic geomorphology of alluvial fans and mountain fronts near Ventura, California. In: Morisawa M (ed) Tectonic geomorphology. Proceedings of the 15th annual geomorphology symposium. Allen and Unwin Publishers, Boston, MA, pp 83–207
Romshoo SA, Bhat SA, Rashid I (2012) Geoinformatics for assessing the morphometric control on hydrological response at watershed scale in the Upper Indus Basin. J Earth Syst Sci 121(3):659–686
Romshoo SA, Altaf S, Rashid I, Dar RA (2017) Climatic, geomorphic and anthropogenic drivers of the 2014 extreme flooding in the Jhelum basin of Kashmir, India. Geomatics, Natural Hazards and Risk 9(1):224–248
Sangireddy H, Carothers RA, Stark CP, Passalacqua P (2016) Controls of climate, topography, vegetation, and lithology on drainage density extracted from high resolution topography data. J Hydrol 537:271–282
Saran S, Sterk G, Peters P, Dadhwal VK (2010) Evaluation of digital elevation models for delineation of hydrological response units in a Himalayan watershed. Geocarto International 25(2):105–122
Schiffman C, Bali BS, Szeliga W, Bilham R (2013) Seismic slip deficit in the Kashmir Himalaya from GPS observations. Geophys Res Lett 40(21):5642–5645
Schneider A, Jost A, Coulon C, Silvestre M, Théry S, Ducharne A (2017) Global-scale river network extraction based on high-resolution topography and constrained by lithology, climate, slope, and observed drainage density. Geophys Res Lett 44(6):2773–2781
Schumm SA (1956) Evolution of drainage systems and slopes in badlands at Perth Amboy, New Jersey. Geol Soc Am Bull 67(5):597–646
Sefercik U, Jacobsen K, Oruc M, Marangoz A (2007) Comparison of spot, SRTM and ASTER DEMs. Proc Int Soc Photogramm Remote Sensing 36(1):W51
Shah AA (2015) Kashmir basin fault and its tectonic significance in NW Himalaya, Jammu and Kashmir. India International Journal of Earth Sciences 104(7):1901–1906
Sharma M, Paige GB, Miller SN (2010) DEM development from ground-based LiDAR data: a method to remove non-surface objects. Remote Sensing 2(11):2629–2642
Shreve RL (1966) Statistical law of stream numbers. J Geol 74(1):17–37
Singh OP (1980) Geomorphology of drainage basins in Palamau upland. Recent Trends and Concepts in Geography 1:229–247
Singh MK, Gupta RD, Bhardwaj A, Ganju A (2016) Scenario-based validation of moderate resolution DEMs freely available for complex Himalayan terrain. Pure Appl Geophys 173(2):463–485
Snow RS, Slingerland RL (1987) Mathematical modeling of graded river profiles. J Geol 95(1):15–33
Strahler AN (1952) Dynamic basis of geomorphology. Geol Soc Am Bull 63(9):923–938
Strahler AN (1957) Quantitative analysis of watershed geomorphology. Eos, Trans Ame Geophys Union 38(6):913–920
Strahler AN (1964) Part II. Quantitative geomorphology of drainage basins and channel networks. Handbook of Applied Hydrology, McGraw-Hill, New York, pp 4–39
Strahler AN (2002) Physical geography: science and systems of the human environment. Wiley, New York
Sung Q, Chen Y (2004) Geomorphic evidence and kinematic model for quaternary transfer faulting of the Pakuashan anticline, Central Taiwan. J Asian Earth Sci 24(3):389–404
Tarboton DG, Shankar U (1998) The identification and mapping of flow networks from digital elevation data. Invited Presentation at AGU Fall Meeting, San Francisco, December 6 to 10.
Thakur VC, Jayangondaperumal R, Malik MA (2010) Redefining Medlicott–Wadia's main boundary fault from Jhelum to Yamuna: an active fault strand of the main boundary thrust in northwest Himalaya. Tectonophysics 489(1–4):29–42
Thomas J, Joseph S, Thrivikramaji KP (2010) Morphometric aspects of a small tropical mountain river system, the southern Western Ghats. India Int J Digital Earth 3(2):135–156
Toutin T (2002) Three-dimensional topographic mapping with ASTER stereo data in rugged topography. IEEE Trans Geosci Remote Sens 40(10):2241–2247
Tucker GE, Bras RL (1998) Hillslope processes, drainage density, and landscape morphology. Water Resour Res 34(10):2751–2764
Tucker GE, Catani F, Rinaldo A, Bras RL (2001) Statistical analysis of drainage density from digital terrain data. Geomorphology 36(3–4):187–202
Turowski JM, Lague D, Hovius N (2009) Response of bedrock channel width to tectonic forcing: Insights from a numerical model, theoretical considerations, and comparison with field data. J Geophys Res: Earth Surf 114(F3). https://doi.org/10.1029/2008JF001133
Verrios S, Zygouri V, Kokkalas S (2004) Morphotectonic analysis in the Eliki fault zone (Gulf of Corinth, Greece). Bull of the Geol Soc of Greece 36(4):1706–1715

Wadia DN (1975) Geology of India, 4th edn. Tata McGraw-Hill, Tenth reprint (1989), New Delhi

Wells SG, Bullard TF, Menges CM, Drake PG, Karas PA, Kelson KI, Ritter JB, Wesling JR (1988) Regional variations in tectonic geomorphology along a segmented convergent plate boundary pacific coast of Costa Rica. Geomorphology 1(3):239–265

Wolock DM, McCabe GJ (2000) Differences in topographic characteristics computed from 100 and 1000 m resolution digital elevation model data. Hydrol Process 14(6):987–1002

Zuchiewicz W (1980) The tectonic interpretation of longitudinal profiles of the Carpathians rivers. Ann Soc Geol Pol 50(3–4):311–328

Publisher's Note Springer Nature remains neutral with regard to jurisdictional claims in published maps and institutional affiliations.